Electronic Supplementary Material (ESI) for Inorganic Chemistry Frontiers.

Supporting Information

for

Tuning the Magnetic Properties of Dinuclear Cobalt-Tetraoxolene Compounds: From Valence Tautomerism to Ferromagnetic Coupling

Yu-Meng Zhao,[a] Jia-Ping Wang,[a] Xiang-Yi Chen,[b] Meng Yu,*[a] Alyona A. Starikova,*[c] and Jun Tao*[a]

[†]Key Laboratory of Cluster Science of Ministry of Education, School of Chemistry and Chemical Engineering, Liangxiang Campus, Beijing Institute of Technology, Beijing 102488, People's Republic of China.

[‡]Fujian Institute for Food and Drug Quality Control, Fuzhou, Fujian 350002, People's Republic of China.

[§]Institute of Physical and Organic Chemistry, Southern Federal University, Stachka Avenue 194/2, Rostov-on-Don 344090, Russian Federation.

Email: taojun@bit.edu.cn; mengyu@bit.edu.cn; aastarikova@sfedu.ru

Contents

1. Additional Tables

Table S1. Frequencies (in cm^{-1}) of stretching vibrations, according to the DFT UTPSSh/6-311++G(d,p) calculations.

Complex	C≡O ($[Co(CO)_4]^-$)	C–N (Me_ntpa)	C–O/C=O (semiquinone)	C–O (catecholate)
3, $\{Co^{III\text{-}LS}$–pyrene$^{Cat\text{-}Sq}$–$Co^{II\text{-}HS}\}^{2+}$	2114 2107 2033 2029 1990 1986 1977 1974	1660 1659 1632 1631	1500	1448
4, $\{Co^{II\text{-}HS}$–pyrene$^{Sq\text{-}Sq}$–$Co^{II\text{-}HS}\}^{2+}$	2109 2029 1985 1977	1661 1660 1633	1496	–
5, $\{Co^{II\text{-}HS}$–pyrene$^{Sq\text{-}Sq}$–$Co^{II\text{-}HS}\}^{2+}$	2109 2030 1986 1978	1661 1659 1634	1497	–

Table S2. Crystal data and structural refinements for **3**.

		3	
T / K	100	298	360
Formula	$C_{82}H_{74}Co_4N_8O_{12}$	$C_{68}H_{58}Co_4N_8O_{12}$	$C_{68}H_{58}Co_4N_8O_{12}$
M_r / g mol^{-1}	1599.21	1414.94	1414.94
Crystal system		Monoclinic	
Space group		$P2_1/c$	
a / Å	8.7470(5)	8.8691(8)	8.9372(4)
b / Å	17.2680(7)	17.7249(14)	17.7258(8)
c / Å	24.2915(1)	24.8969(18)	24.7614(10)
α / °	90	90	90
β / °	92.161(4)	91.742(8)	92.352(4)
γ / °	90	90	90
V / Å^3	3666.5(3)	3912.1(5)	3919.4(3)
Z		2	
ρ_{calc} / g cm^{-3}	1.449	1.201	1.199
μ / mm^{-1}	0.959	0.890	0.888
F(000)	1652.0	1452.0	1452.0
R_{int} / %	7.34	7.15	3.86
R_1 [$I \geq 2\sigma(I)$]	0.0732	0.0760	0.0738
wR_2 (all data)	0.1936	0.2270	0.2432
CCDC no.	2224738	2224741	2224744

Table S3. Selected bond lengths and angles for **3**.

	3		
T / K	100	298	360
Co1-O1 / Å	1.868(2)	1.896(3)	1.976(3)
Co1-O2 / Å	1.879(3)	1.930(3)	1.933(3)
Co1-N1 / Å	1.965(3)	2.008(3)	2.061(4)
Co1-N2 / Å	1.925(3)	1.968(3)	2.008(4)
Co1-N3 / Å	1.920(3)	1.971(3)	2.016(4)
Co1-N4 / Å	1.922(3)	1.968(3)	1.997(4)
O1-C1 / Å	1.358(4)	1.342(4)	1.301(6)
O2-C2 / Å	1.352(4)	1.330(4)	1.327(5)
C1-C2 / Å	1.380(5)	1.402(5)	1.400(6)
C1-C5 / Å	1.430(5)	1.428(5)	1.450(6)
C2-C3 / Å	1.438(5)	1.432(5)	1.414(6)
C3-C4 / Å	1.426(5)	1.410(5)	1.421(5)
C4-C4 / Å	1.427(5)	1.428(4)	1.441(6)
C4-C5 / Å	1.423(4)	1.421(4)	1.420(6)
N2-Co1-N1	85.62(1)	83.58(1)	82.16(2)
N2-Co1-N3	170.0(7)	166.5(1)	163.4(1)
N3-Co1-N1	84.73(1)	83.06(1)	81.67(1)
N4-Co1-N1	86.12(1)	84.01(1)	83.08(1)
N4-Co1-N2	92.19(1)	91.66(1)	88.88(1)
N4-Co1-N3	89.89(1)	89.12(1)	92.68(1)
O1-Co1-N1	178.6(1)	178.6(1)	179.1(1)
O1-Co1-N2	95.00(1)	97.05(1)	87.88(2)
O1-Co1-N3	94.71(1)	96.33(1)	98.54(1)
O1-Co1-N4	92.57 (1)	94.78(1)	96.10(1)
O2-Co1-N1	91.78(1)	94.50(1)	96.17(1)
O2-Co1-N2	89.38(1)	90.39(1)	87.82(1)
O2-Co1-N3	88.19(1)	88.47(1)	90.39(1)
O2-Co1-N4	177.28(1)	177.3(1)	176.6(1)
O2-Co1-O1	89.50(1)	86.69(1)	84.62(1)
Σ / deg[a]	32.81	49.76	63.32
Θ / deg[b]	88.85	135.9	175.6
Diox MOS[c]	-1.8	-1.6	-1.4

[a]The sum of the deviation of 12 unique *cis* ligand-metal-ligand angles from 90°. [b]The sum of the deviation of 24 unique torsional angles between the ligand atoms on opposite triangular faces of the octahedron viewed along the *pseudo*-threefold axis from 60°. [c]Empirical metrical oxidation state of tetraoxolene ligands, proposed by Brown et al. uses a least-squares fitting of C–C and C–O bond lengths to assign an apparent oxidation state: −1 for a semiquinonate ligand and −2 for a catecholate ligand.

Table S4. Bond valence sum (BVS)[a] calculation for Co atoms in **3**.

		3	
T / K	100	298	360
Atom	Co1	Co1	Co1
BVS	3.1	2.8	2.5

Table S5. Crystal data and structural refinements for **4** and **5**.

	4	**5**
T / K	100	100
Formula	$C_{70}H_{62}Co_4N_8O_{12}$	$C_{74}H_{68}Co_4Cl_6N_8O_{12}$
M_r / g mol^{-1}	1442.99	1709.78
Crystal system	Monoclinic	Triclinic
Space group	$P2_1/c$	$P\bar{1}$
a / Å	14.477(2)	11.8002(5)
b / Å	15.1685(7)	12.6052(7)
c / Å	24.167(3)	16.1129(8)
α / °	90	103.951(4)
β / °	135.18(3)	97.024(4)
γ / °	90	106.222(4)
V / Å^3	3740.7(14)	2186.65(19)
Z	2	1
ρ_{calc} / g cm^{-3}	1.281	1.298
μ / mm^{-1}	0.932	0.985
F(000)	1484.0	874.0
R_{int} / %	5.88	6.80
R_1 [$I \geq 2\sigma(I)$]	0.1286	0.0774
wR_2 (all data)	0.3994	0.2308
CCDC no.	2287990	2158906

Table S6. Selected bond lengths and angles for **4** and **5**.

	4	**5**
T / K	100	100
Co1-O1 / Å	2.006(6)	2.015(3)
Co1-O2 / Å	2.076(8)	2.129(2)
Co1-N1 / Å	2.130(7)	2.160(4)
Co1-N2 / Å	2.150(3)	2.151(4)
Co1-N3 / Å	2.146(4)	2.186(3)
Co1-N4 / Å	2.074(6)	2.186(3)
O1-C1 / Å	1.274(9)	1.291(4)
O2-C2 / Å	1.290(7)	1.272(4)
C1-C2 / Å	1.454(8)	1.448(5)
C1-C5 / Å	1.454(8)	1.449(5)
C2-C3 / Å	1.435(1)	1.461(5)
C3-C4 / Å	1.421(8)	1.416(5)
C4-C4' / Å	1.423(1)	1.449(5)
C4-C5 / Å	1.41(1)	1.416(5)
N2-Co1-N1	78.64(2)	77.08(1)
N2-Co1-N3	155.4(1)	155.1(1)
N3-Co1-N1	77.17(2)	79.47(1)
N4-Co1-N1	82.13(2)	80.81(1)
N4-Co1-N2	85.36(1)	99.42(1)
N4-Co1-N3	95.75(2)	84.96(1)
O1-Co1-N1	175.4(2)	174.1(1)
O1-Co1-N2	105.6(1)	105.3(1)
O1-Co1-N3	98.70(2)	97.23(1)
O1-Co1-N4	96.28(2)	103.9 (1)
O2-Co1-N1	101.1(2)	94.88(1)
O2-Co1-N2	89.42(1)	87.36(1)
O2-Co1-N3	90.80(2)	86.34(1)
O2-Co1-N4	173.2(1)	171.8(1)
O2-Co1-O1	80.97(17)	79.97(1)
Σ / deg[a]	94.58	104.8
Θ / deg[b]	285.5	267.1
Diox MOS[c]	-1.05	-0.96

[a]The sum of the deviation of 12 unique *cis* ligand-metal-ligand angles from 90°. [b]The sum of the deviation of 24 unique torsional angles between the ligand atoms on opposite triangular faces of the octahedron viewed along the *pseudo*-threefold axis from 60°. [c]Empirical metrical oxidation state of tetraoxolene ligands, proposed by Brown et al. uses a least-squares fitting of C–C and C–O bond lengths to assign an apparent oxidation state: −1 for a semiquinonate ligand and −2 for a catecholate ligand.

Table S7. Bond valence sum (BVS)[a] calculation for Co atoms in **4** and **5**.

	4	**5**
T / K	100	100
Atom	Co1	Co1
BVS	1.9	1.7

Table S8. Parameters of intermolecular interactions for **3**.

	3					
T / K	100		298		360	
	lengths / Å	angles / deg.	lengths / Å	angles / deg.	lengths / Å	angles / deg.
π···π / Å	3.867	-	3.944	-	4.008	-
C–H···π / Å	3.554	156.7	3.735	151.7	3.785	151.9

Table S9. Parameters Obtained from PHI Fitting for compounds **4** and **5** using two other fitting models.

	PHI fitting		PHI fitting	
	4	**5**	**4**	**5**
g_{Co}	2.10	2.00	2.04	2.00
$D\ (\mathrm{cm}^{-1})$	45.0	28.6	59.7	24.0
$J\ (\mathrm{cm}^{-1})$	32.8	150	121.2	137.7
$J_1\ (\mathrm{cm}^{-1})$	51.4	43.6	63.2	56.7
$J_2\ (\mathrm{cm}^{-1})$	–	–	-4.6	-3.5
$J_3\ (\mathrm{cm}^{-1})$	–	–	-0.8	0.0
$zJ'\ (\mathrm{cm}^{-1})$	–	–	–	–
$TIP\ (\mathrm{cm}^3\ mol^{-1})$	3.6×10^{-4}	5.7×10^{-4}	–	–

Table S10. Spin states (S), total energies without (E) and with (E^{ZPE}) zero-point harmonic vibrations, total enthalpies (H^{298}) and expectation values of the spin-squared operator ($\hat{S}^2$) of the compounds **3** -**5** calculated by the DFT UTPSSh/6-311++G(d,p) method.

Charge Distribution	S	E, a.u.	E^{ZPE}, a.u.	H^{298}, a.u.	$\hat{S}^2$
Compound **3**					
{ls-Co^{III}(tpa)–$pyrene^{Cat\text{-}Cat}$–ls-Co^{III}(tpa)}	0	-9499.602610	-9498.462301	-9498.380696	0.000
{ls-Co^{III}(tpa)–$pyrene^{Cat\text{-}Sq}$–hs-Co^{II}(tpa)}	2	-9499.598192	-9498.461007	-9498.376493	6.016

βα [a]	1	-9499.596922	–	–	2.988
{hs-Co^{II}(tpa)–$pyrene^{Sq\text{-}Sq}$–hs-Co^{II}(tpa)}	4	-9499.590856	-9498.457531	-9498.373622	20.032
αββα	2	-9499.587535	–	–	7.984
ααββ	0	-9499.589450	–	–	4.004
αβαβ	0	-9499.586315	–	–	3.949
αβαα	3	-9499.587840	–	–	12.975
βααα	1	-9499.589286	–	–	5.009
Compound **4**					
{ls-Co^{III}(Metpa)–$pyrene^{Cat\text{-}Cat}$–ls-Co^{III}(Metpa)}	0	-9578.256293	-9577.060359	-9576.974602	0.000
{ls-Co^{III}(Metpa)–$pyrene^{Cat\text{-}Sq}$–hs-Co^{II}(Metpa)}	2	-9578.257212	-9577.064794	-9576.976897	6.016
βα	1	-9578.255285	–	–	3.005
{hs-Co^{II}(Metpa)–$pyrene^{Sq\text{-}Sq}$–hs-Co^{II}(Metpa)}	4	-9578.255743	-9577.066804	-9576.977053	20.031
αββα	2	-9578.250746	–	–	8.013
ααββ	0	-9578.253419	–	–	4.003
αβαβ	0	-9578.249333	–	–	3.974
αβαα	3	-9578.251560	–	–	12.991
βααα	1	-9578.252957	–	–	5.023
Compound **5**					
{ls-Co^{III}(Me_2tpa)–$pyrene^{Cat\text{-}Cat}$–ls-Co^{III}(Me_2tpa)}	0	-9656.900813	-9655.649592	-9655.561084	0.000
{ls-Co^{III}(Me_2tpa)–$pyrene^{Cat\text{-}Sq}$–hs-Co^{II}(Me_2tpa)}	2	-9656.909564	-9655.661944	-9655.572274	6.016
βα	1	-9656.907611	–	–	3.010
{hs-Co^{II}(Me_2tpa)–$pyrene^{Sq\text{-}Sq}$–hs-Co^{II}(Me_2tpa)}	4	-9656.915134	-9655.671404	-9655.579476	20.031
αββα	2	-9656.911122	–	–	8.019
ααββ	0	-9656.913667	–	–	4.002
αβαβ	0	-9656.908457	–	–	3.837
αβαα	3	-9656.911670	–	–	12.992
βααα	1	-9656.913139	–	–	5.024

[a] α corresponds to spin-up, β corresponds to spin-down; the order of the paramagnetic centers in {Co^{II}–$pyrene^{Sq\text{-}Sq}$–Co^{II}} charge distributions: (1) hs-Co^{II} (2) Sq (3) Sq (4) hs-Co^{II}

Table S11. Relative energies without (ΔE) and with (E^{ZPE}) zero-point harmonic vibrations, relative enthalpies (ΔH^{298}) (all values are given in kcal mol^{-1}) of charge distributions of the compounds **3**-**5** calculated by the DFT UTPSSh/6-311++G(d,p) method.

Charge Distribution		ΔE	E^{ZPE}	H^{298}
3	{ls-Co^{III}(tpa)–$pyrene^{Cat\text{-}Cat}$–ls-Co^{III}(tpa)}	0.0	0.0	0.0
	{ls-Co^{III}(tpa)–$pyrene^{Cat\text{-}Sq}$–hs-Co^{II}(tpa)}	2.8	0.8	2.6
	{hs-Co^{II}(tpa)–$pyrene^{Sq\text{-}Sq}$–hs-Co^{II}(tpa)}	7.4	3.0	4.4
4	{ls-Co^{III}(Metpa)–$pyrene^{Cat\text{-}Cat}$–ls-Co^{III}(Metpa)}	0.6	4.0	1.5
	{ls-Co^{III}(Metpa)–$pyrene^{Cat\text{-}Sq}$–hs-Co^{II}(Metpa)}	0.0	1.3	0.1
	{hs-Co^{II}(Metpa)–$pyrene^{Sq\text{-}Sq}$–hs-Co^{II}(Metpa)}	0.9	0.0	0.0
5	{ls-Co^{III}(Me_2tpa)–$pyrene^{Cat\text{-}Cat}$–ls-Co^{III}(Me_2tpa)}	9.0	13.7	11.5
	{ls-Co^{III}(Me_2tpa)–$pyrene^{Cat\text{-}Sq}$–hs-Co^{II}(Me_2tpa)}	3.5	5.9	4.5
	{hs-Co^{II}(Me_2tpa)–$pyrene^{Sq\text{-}Sq}$–hs-Co^{II}(Me_2tpa)}	0.0	0.0	0.0

Table S12. Exchange coupling parameters (J, given in cm^{-1}) in the compounds **3**-**5** calculated by the DFT UTPSSh/6-311++G(d,p) method.

Charge Distribution	J (hs-Co^{II}-Sq1)[a]	J (hs-Co^{II}-Sq2)	J (Sq1-Sq2)	J (hs-Co^{II}-hs-Co^{II})
Compound **3**				
{ls-Co^{III}(tpa)–pyrene^{Cat-Sq}–hs-Co^{II}(tpa)}	92	–	–	–
{hs-Co^{II}(tpa)–pyrene^{Sq-Sq}–hs-Co^{II}(tpa)}	59	2	147	–1
Compound **4**				
{ls-Co^{III}(Metpa)–pyrene^{Cat-Sq}–hs-Co^{II}(Metpa)}	140	–	–	–
{hs-Co^{II}(Metpa)–pyrene^{Sq-Sq}–hs-Co^{II}(Metpa)}	83	8	173	3
Compound **5**				
{ls-Co^{III}(Me_2tpa)–pyrene^{Cat-Sq}–hs-Co^{II}(Me_2tpa)}	143	–	–	–
{hs-Co^{II}(Me_2tpa)–pyrene^{Sq-Sq}–hs-Co^{II}(Me_2tpa)}	83	-11	181	4

[a] Sq1 represents the closest (coordinating) dioxolene and Sq2 represents the dioxolene on the other side of pyrene.

3. Additional Figures

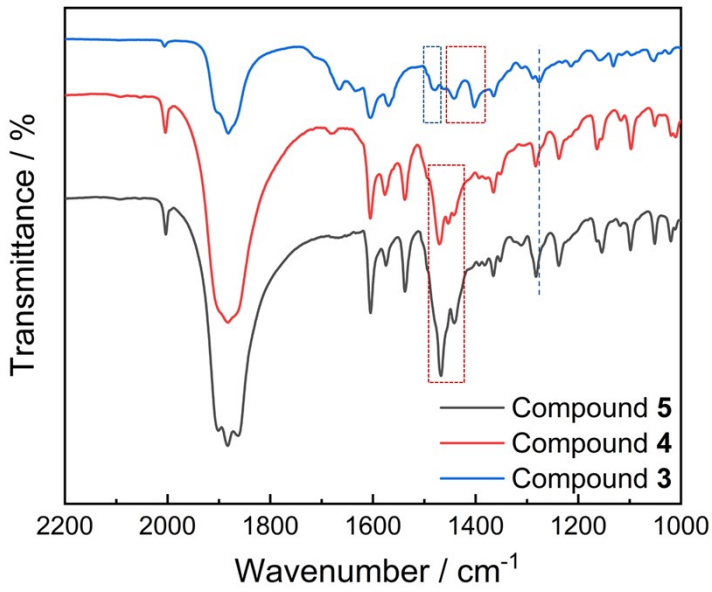

Figure S1. IR spectra of **3**-**5**.

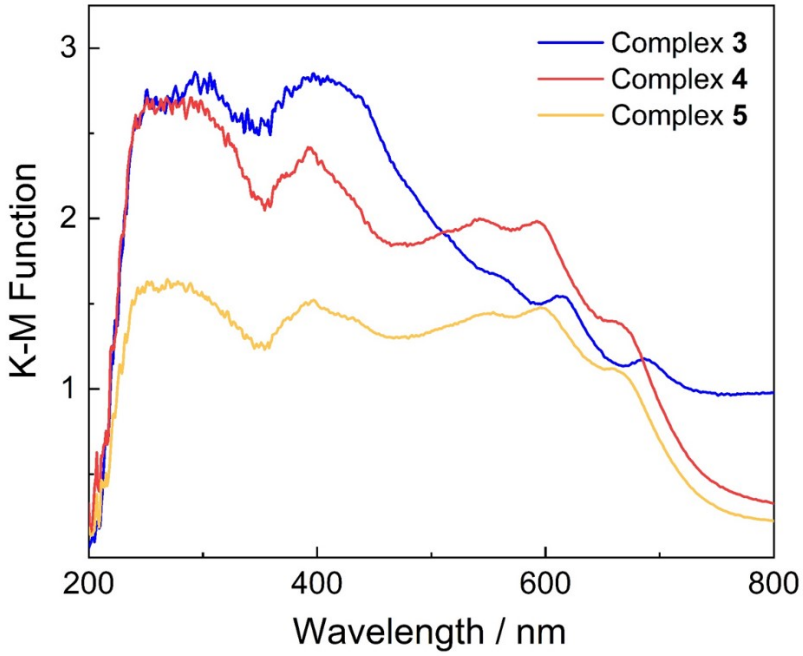

Figure S2. Solid-state UV-Vis diffuse reflectance spectra of **3**-**5**.

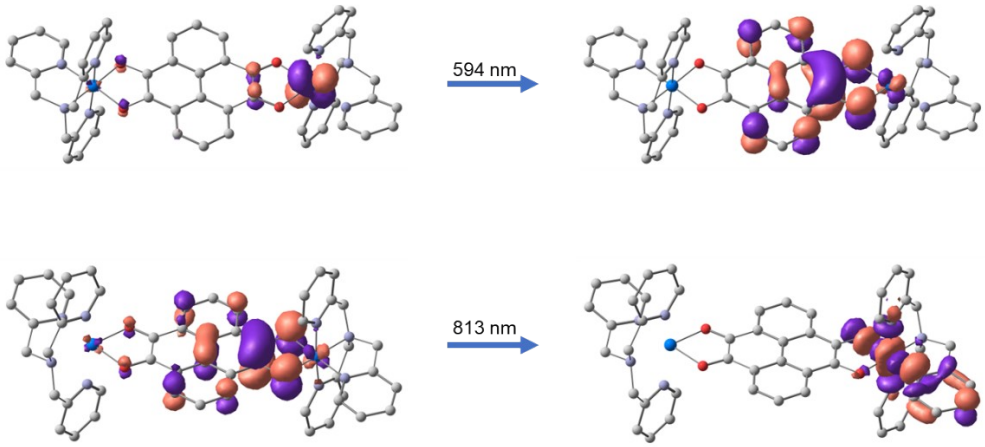

Figure S3. Corresponding orbitals for Compound **3** in electronic absorption spectroscopy**,** as calculated by the TD-DFT method at UTPSSh/def2-SVP level of theory with CPCM (acetonitrile) solvent model. The top one at 594 nm corresponds to a MLCT transition from $Co^{II\text{-}HS}$ to the π* orbital of the semiquinone. The bottom one at 813 nm can be assigned to a LMCT transition. Note that the calculation was conducted for the $\{Co^{III\text{-}LS}\text{–pyrene}^{Cat\text{-}Sq}\text{–}Co^{II\text{-}HS}\}^{2+}$ electronic state.

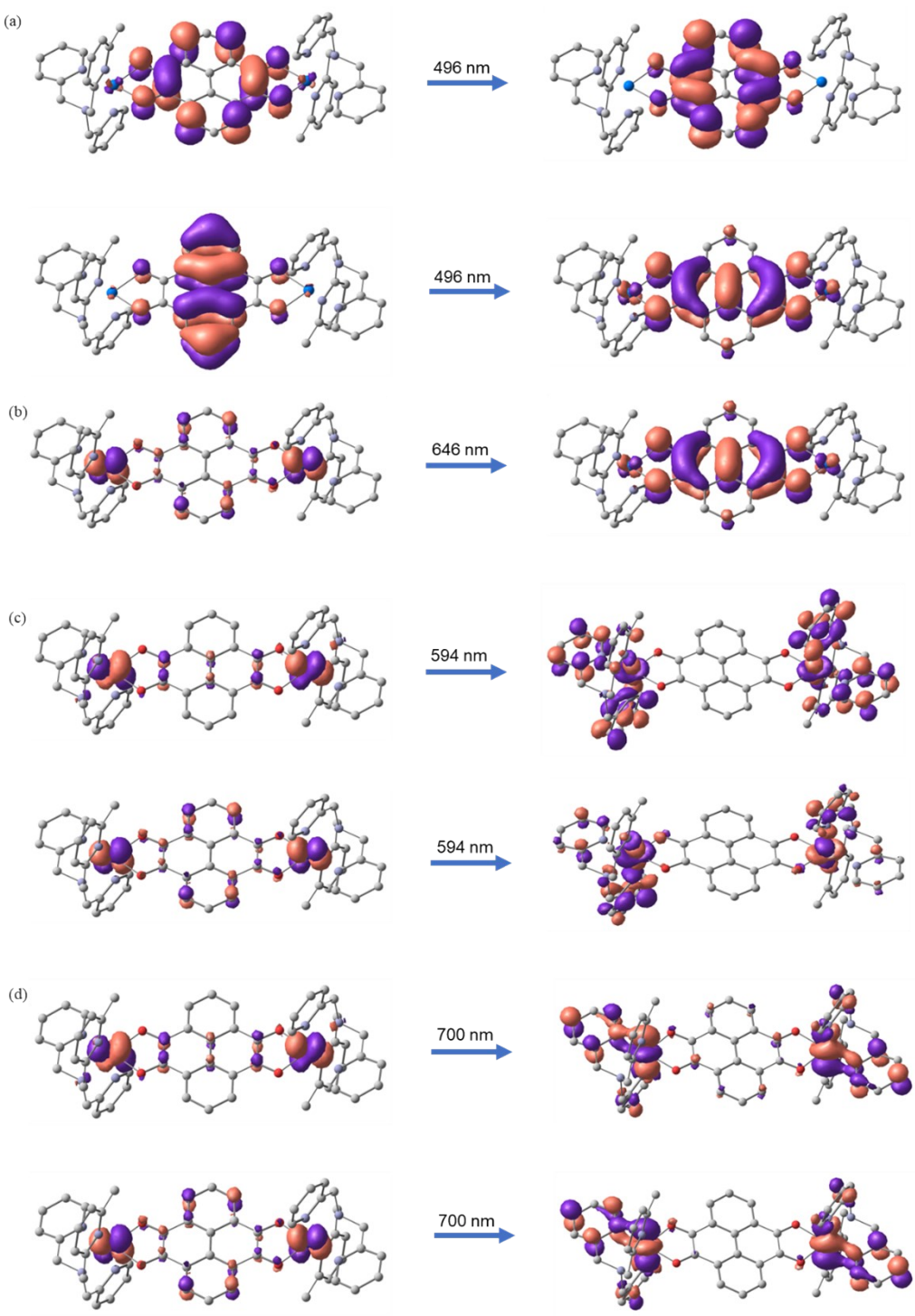

Figure S4. Corresponding orbitals for Compound **4** in electronic absorption spectroscopy**,** as calculated by the TD-DFT method at UTPSSh/def2-SVP level of theory with CPCM (acetonitrile) solvent model. (a) 496 nm transition corresponds to internal semiquinone ligand transitions within the pyrene$^{Sq\text{-}Sq}$ ligand; (b) 646 nm transition can be assigned to a MLCT transitions from Co$^{II\text{-}HS}$ to the π* orbital of semiquinone; (c) 594 nm and (d) 700 nm transitions can be assigned to MLCT transitions from Co$^{II\text{-}HS}$ to the π* orbital of MeTPA. Note that the calculation was conducted for the {Co$^{II\text{-}HS}$–pyrene$^{Sq\text{-}Sq}$–Co$^{II\text{-}HS}$}$^{2+}$ electronic state.

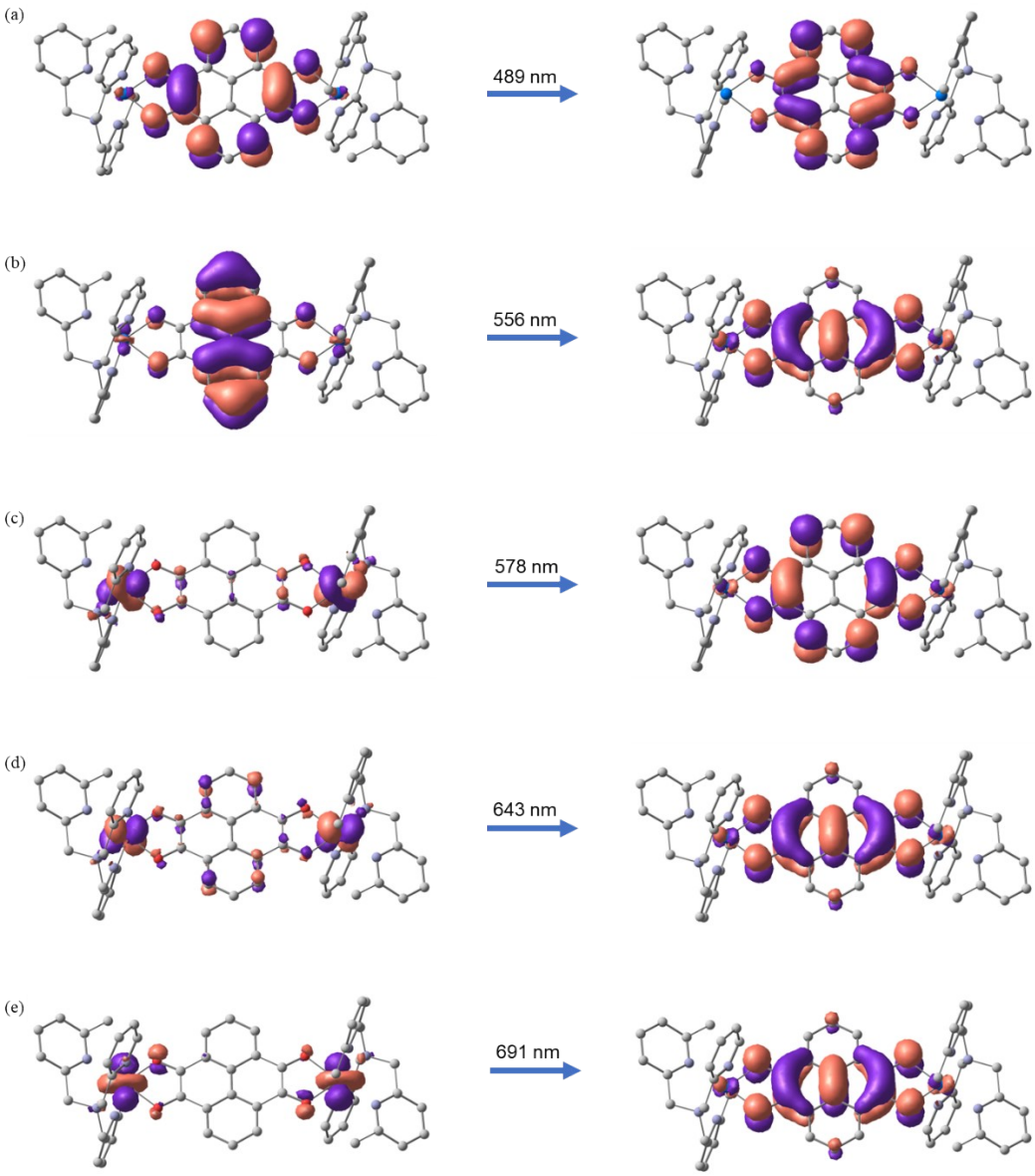

Figure S5. Corresponding orbitals for Compound **5** in electronic absorption spectroscopy**,** as calculated by the TD-DFT method at UTPSSh/def2-SVP level of theory with CPCM (acetonitrile) solvent model. (a) 496 nm and (b) 556 nm transitions correspond to internal semiquinone ligand transitions within the pyrene$^{Sq\text{-}Sq}$ ligand; (c) 556 nm, (d) 643 nm, and (e) 691 nm transitions can be assigned to MLCT transitions from Co$^{II\text{-}HS}$ to the π* orbital of semiquinone. Note that the calculation was conducted for the {Co$^{II\text{-}HS}$–pyrene$^{Sq\text{-}Sq}$–Co$^{II\text{-}HS}$}$^{2+}$ electronic state.

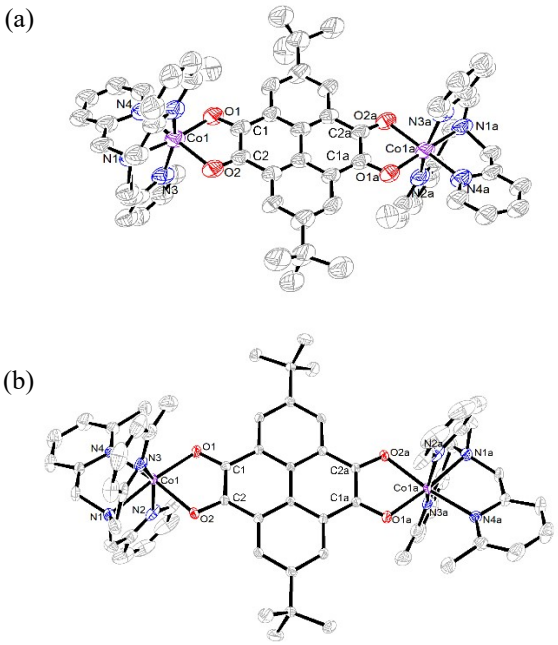

Figure S6. Perspective view of the dinuclear cations of **4** (a) and **5** (b) with 50% thermal ellipsoids. Hydrogen atoms, solvent molecules, and counter-ions are omitted for clarity. Symmetry codes: a) 1 – *x*, 1 – *y*, 2 – *z*; b) – *x*, 2 – *y*, 2 – *z*.

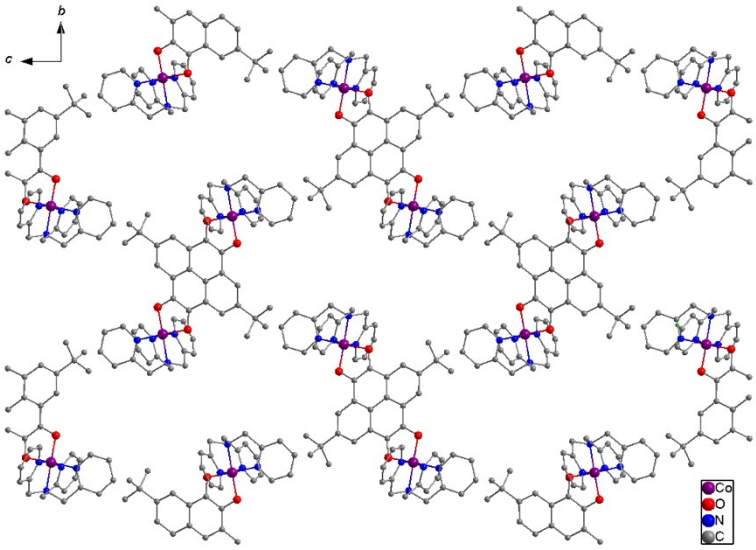

Figure S7. The packing diagram of **3**. Hydrogen atoms, anions, and guest solvent molecules are omitted for clarity.

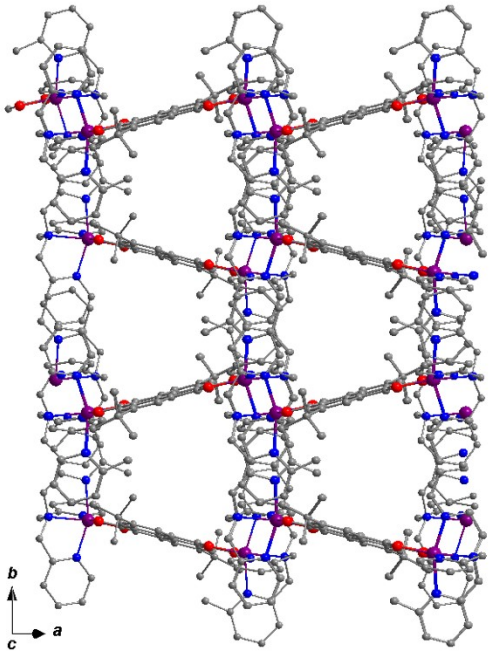

Figure S8. The packing diagrams of **4**. color code: Co, purple; O, red; N, blue; C, grey.

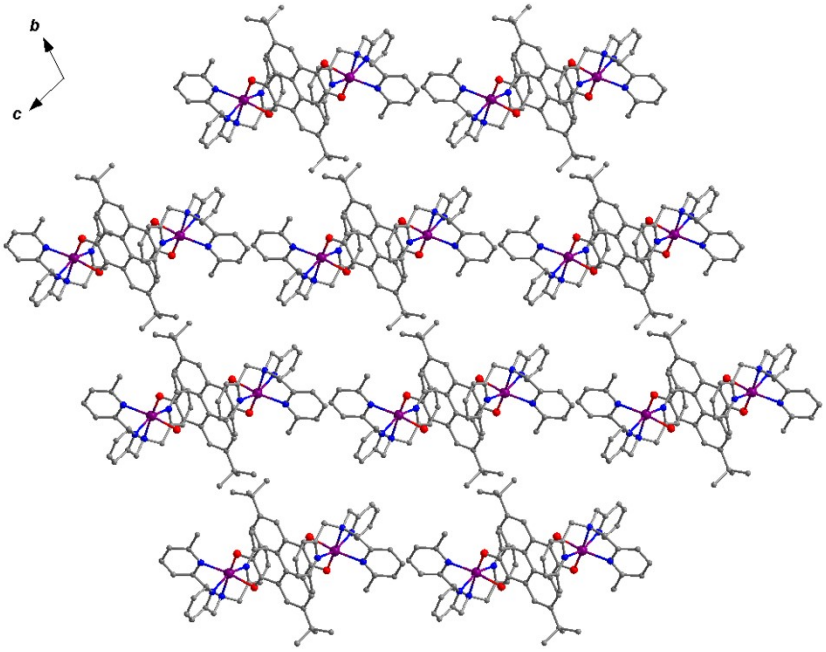

Figure S9. The packing diagrams of **5**. color code: Co, purple; O, red; N, blue; C, grey.

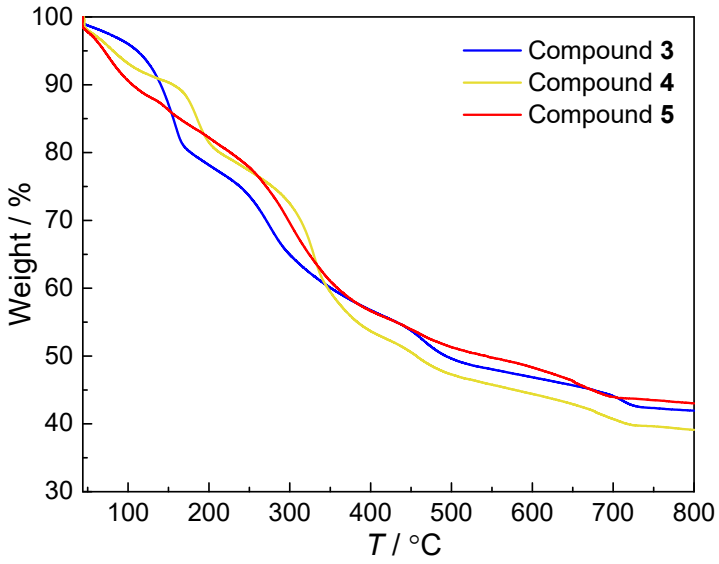

Figure S10. Thermogravimetric analysis of **3** -**5**.

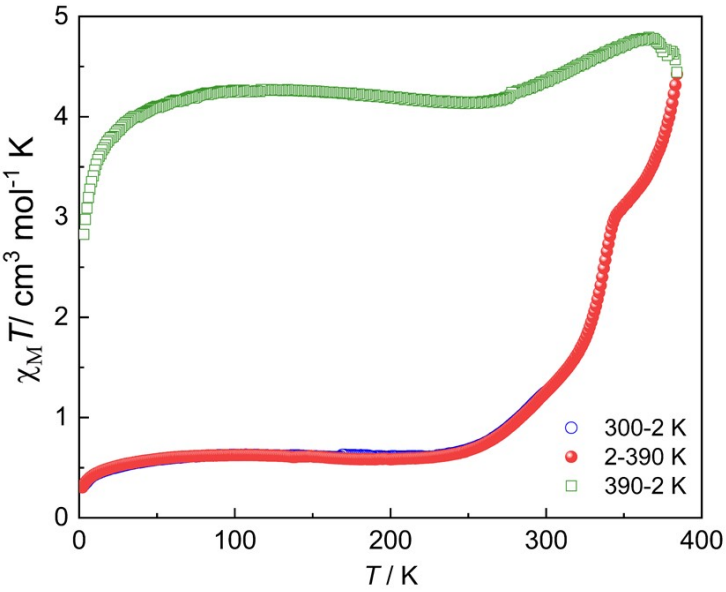

Figure S11. $\chi_M T$ versus T plot for compound **3** in the range of 300-2-390-2 K. Applied field: 5000 Oe.

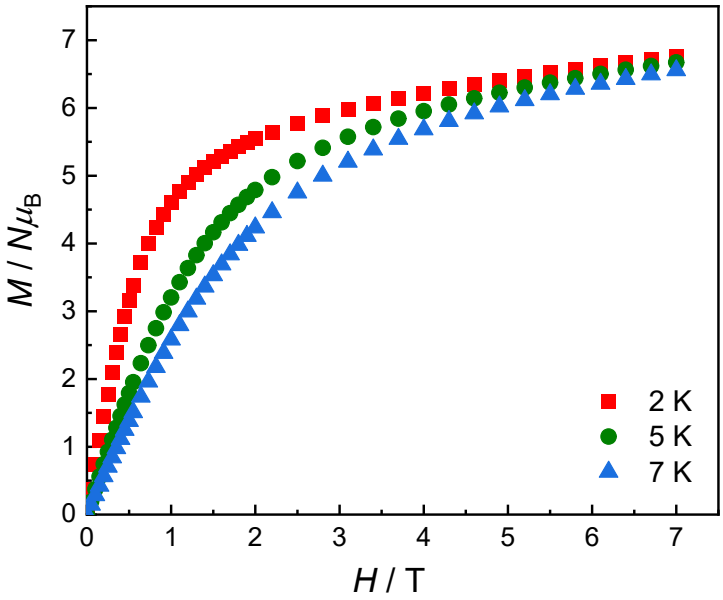

Figure S12. M versus H plots at 2 K, 5 K and 7 K for **4**.

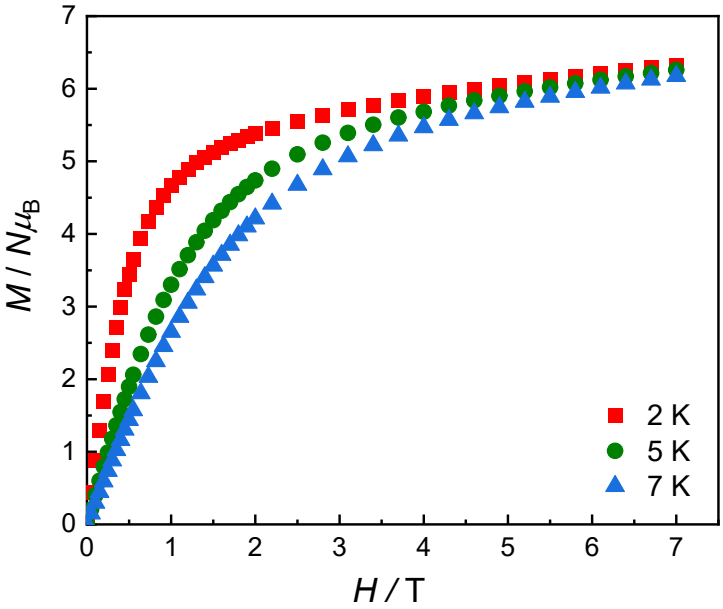

Figure S13. M versus H plots at 2 K, 5 K and 7 K for **5**.

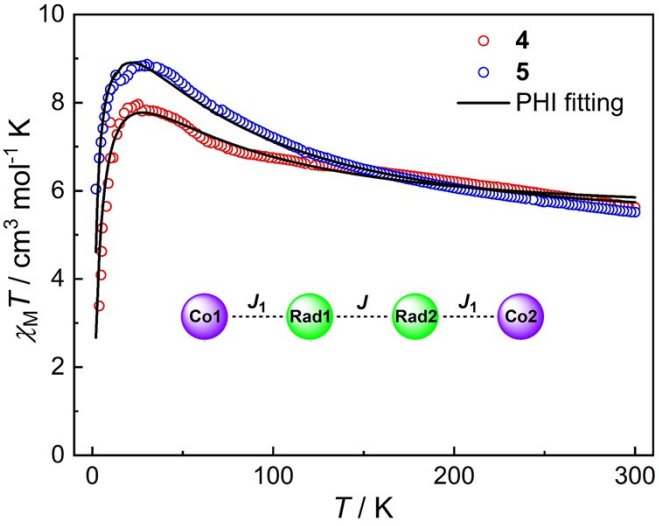

Figure S14. Magnetic susceptibilities of compounds **4** and **5** under applied field of 5000 Oe. Solid black lines represent the fitting results by the PHI program neglecting intermolecular magnetic interactions based on equation 1. Inset: the magnetic coupling parameters of **4** and **5**. Large inconsistency in *J* coupling value was observed between **4** and **5** using this fitting model.

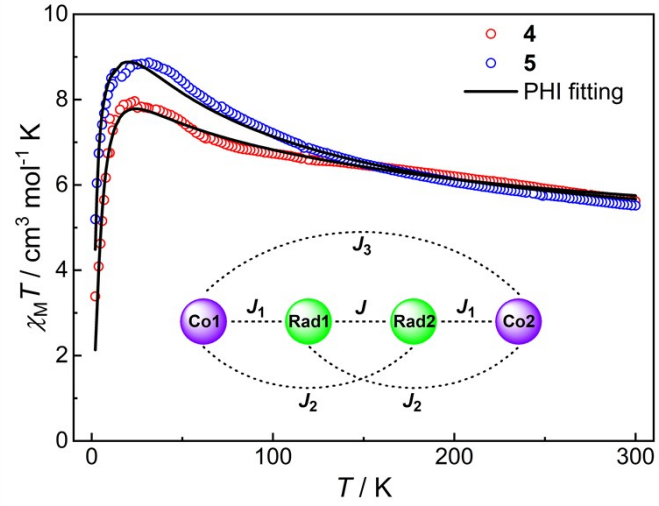

Figure S15. Magnetic susceptibilities of compounds **4** and **5** under applied field of 5000 Oe. Solid black lines represent the fitting results by the PHI program based on equation 1 including long-distance coupling constants J_2 and J_3 during data fitting. Inset: the magnetic coupling parameters of **4** and **5**. A very large *D* value (59.7 cm^{-1}) was used during data fit for compound **4**, which is unlikely.

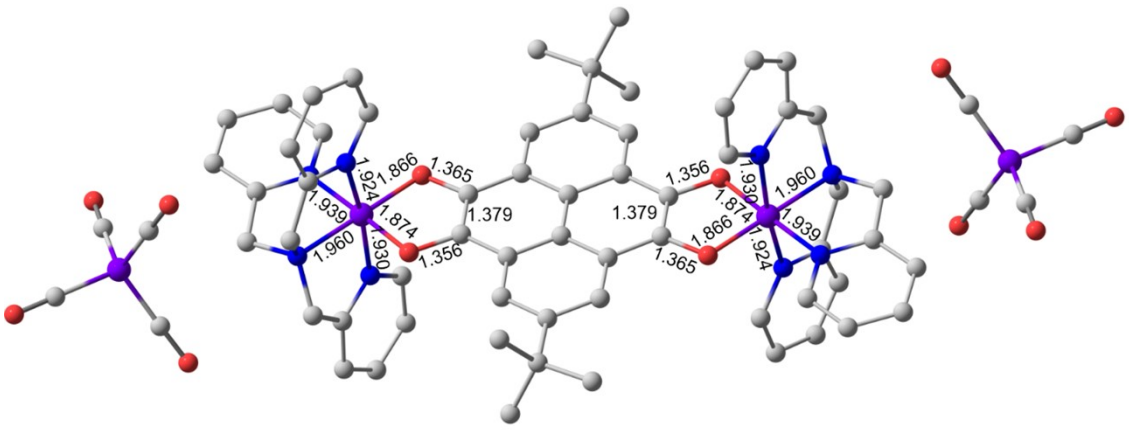

{ls-Co^{III}(tpa)–pyrene$^{Cat\text{-}Cat}$–ls-Co^{III}(tpa)}

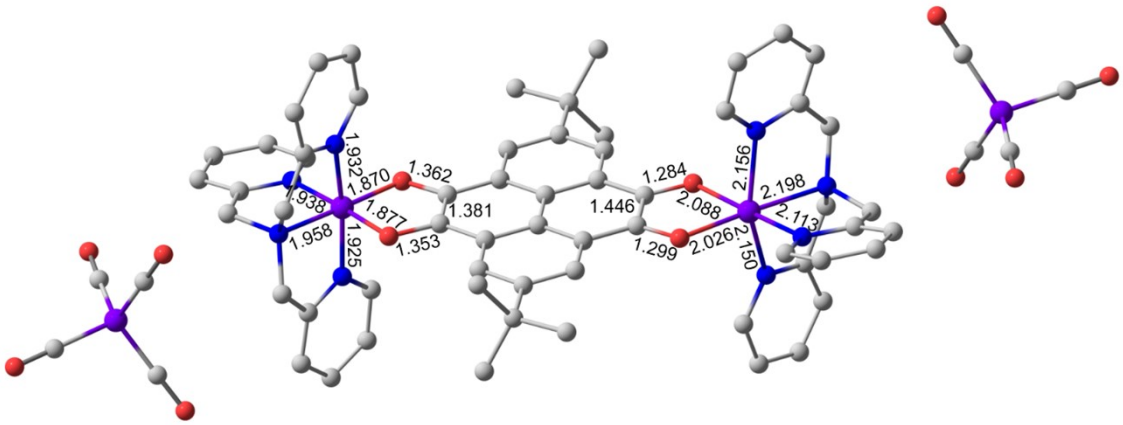

{ls-Co^{III}(tpa)–pyrene$^{Cat\text{-}Sq}$–hs-Co^{II}(tpa)}

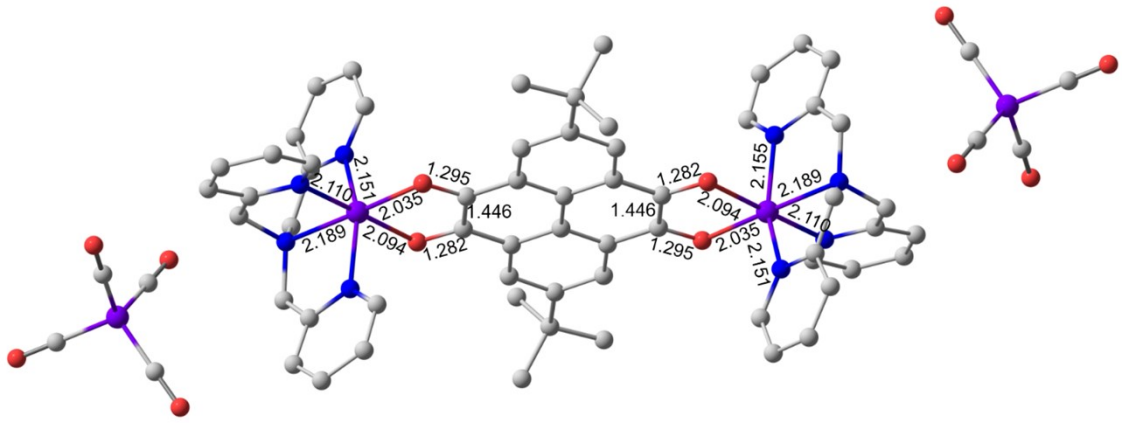

{hs-Co^{II}(tpa)–pyrene$^{Sq\text{-}Sq}$–hs-Co^{II}(tpa)}

Figure S16. Optimized geometries of the compound **3** in the three charge distributions, as calculated by the DFT UTPSSh/6-311++G(d,p) method. Here and in **Figures S17** – **S20**hydrogen atoms are omitted for clarity.

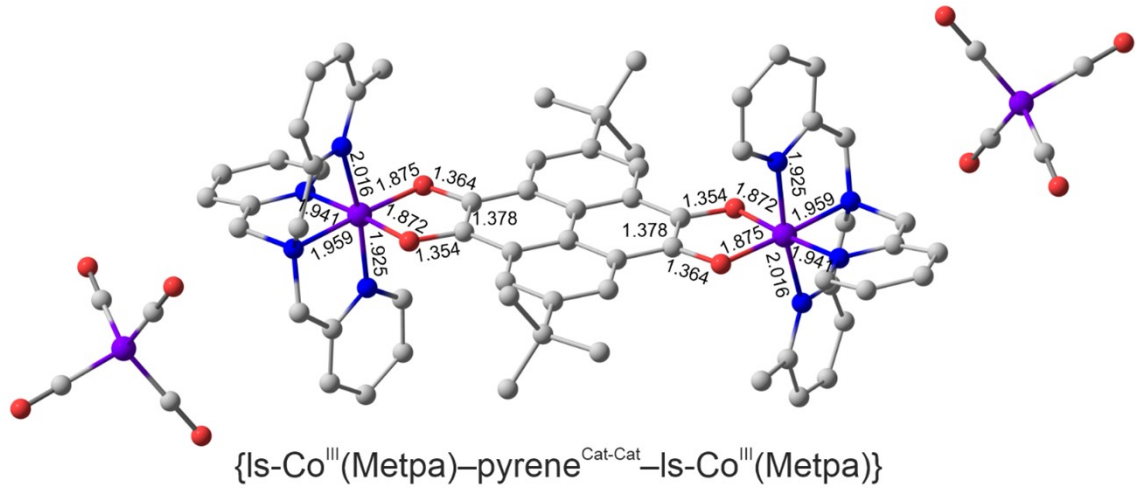

{ls-Co^{III}(Metpa)–pyrene$^{Cat\text{-}Cat}$–ls-Co^{III}(Metpa)}

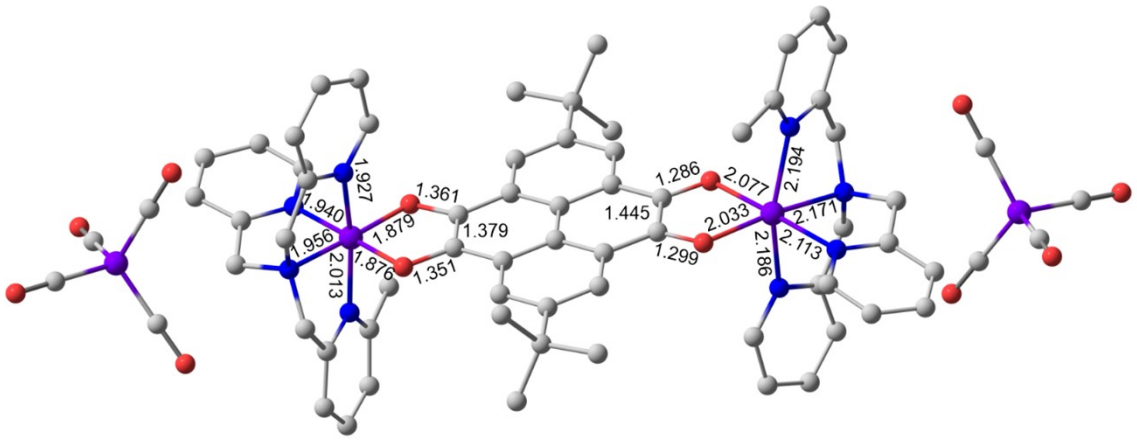

{ls-Co^{III}(Metpa)–pyrene$^{Cat\text{-}Sq}$–hs-Co^{II}(Metpa)}

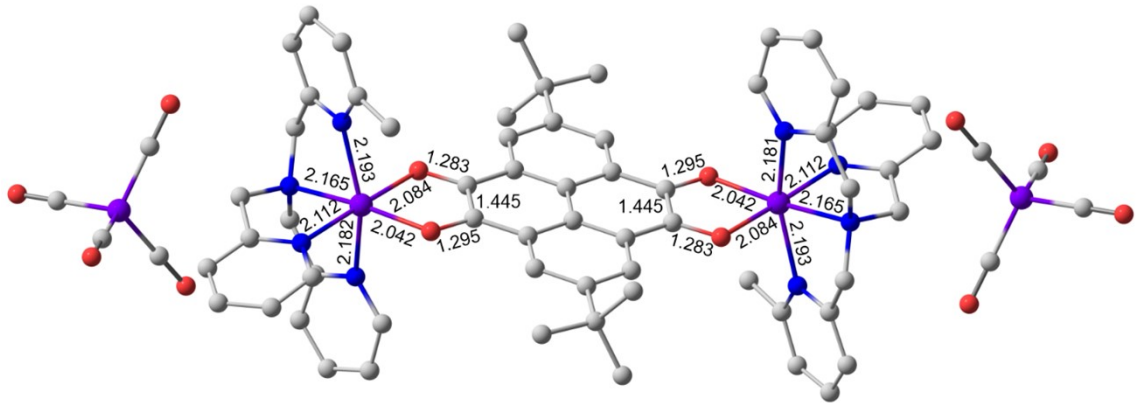

{hs-Co^{II}(Metpa)–pyrene$^{Sq\text{-}Sq}$–hs-Co^{II}(Metpa)}

Figure S17. Optimized geometries of the compound **4** in the three charge distributions, as calculated by the DFT UTPSSh/6-311++G(d,p) method.

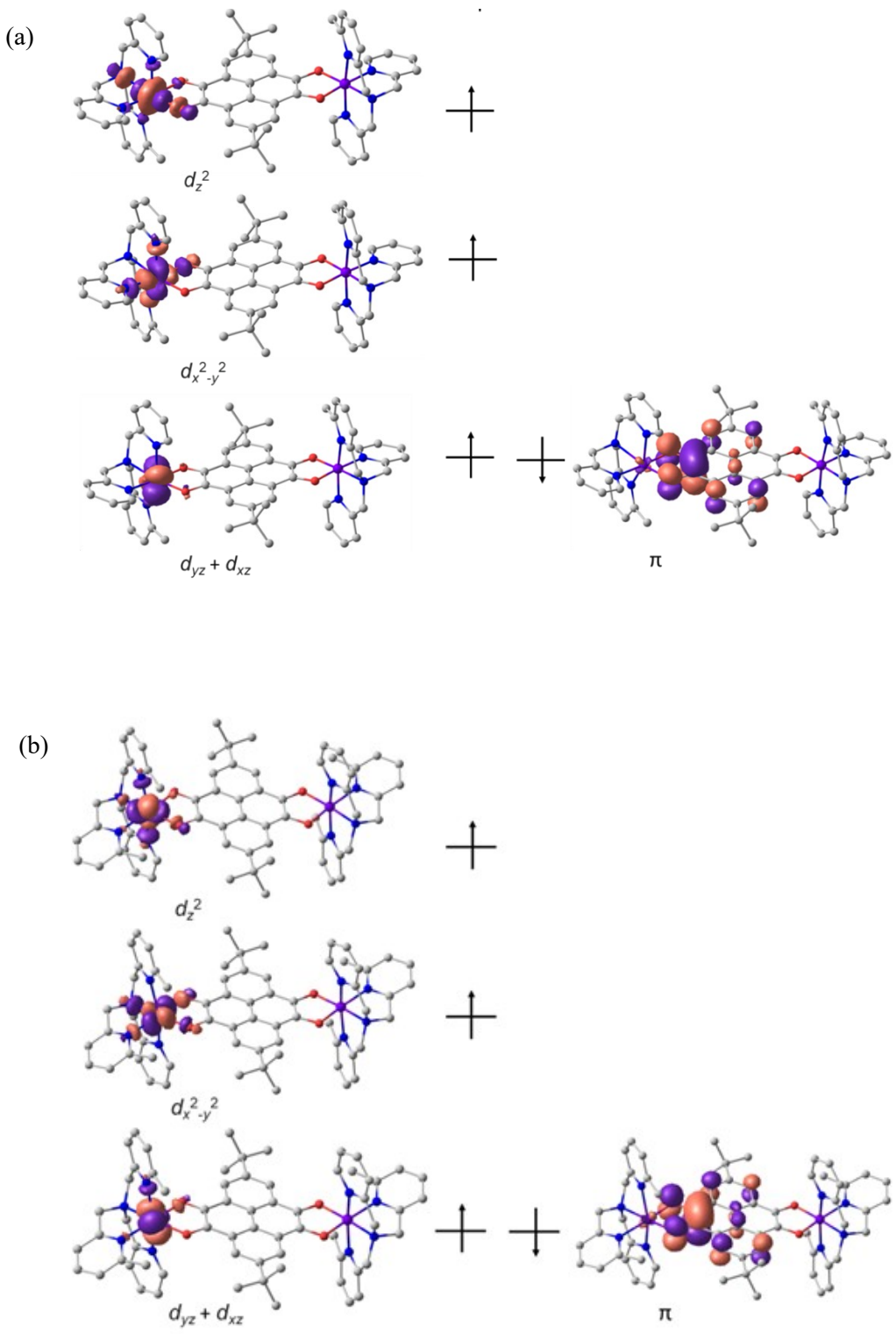

Figure S18. Corresponding orbitals for **4** (a) and **5** (b) visualizing the $Co^{II\text{-}HS}$-Sq1 exchange interactions, as calculated by the DFT UTPSSh/6-311++G(d,p) method (contour value = 0.03 e $Å^{-3}$).

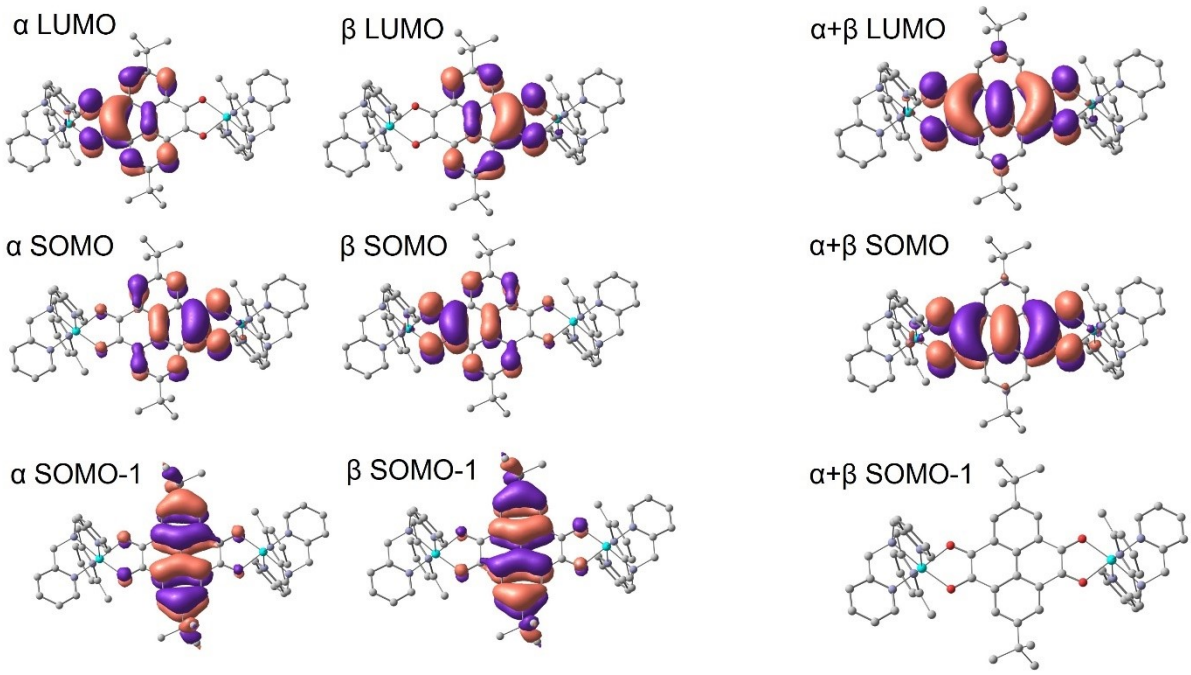

Figure S19. Corresponding orbitals for Zn-SQ-SQ-Zn analogs of **4** and **5** visualizing the $Co^{II\text{-}HS}$-Sq1 exchange interactions, as calculated by the DFT UTPSSh/6-311++G(d,p) method (contour value = 0.03 e $Å^{-3}$).

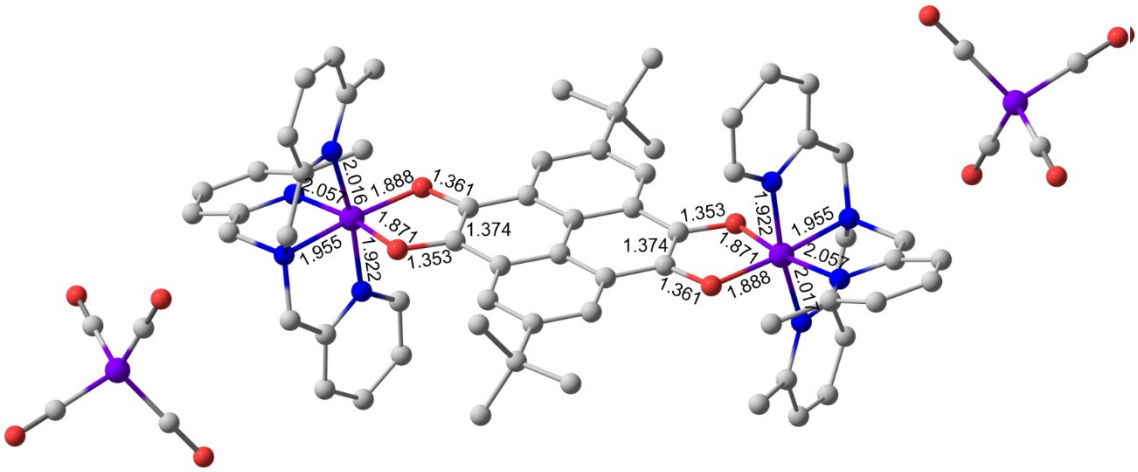

{ls-Co^{III}(Me_2tpa)–pyrene$^{Cat-Cat}$–ls-Co^{III}(Me_2tpa)}

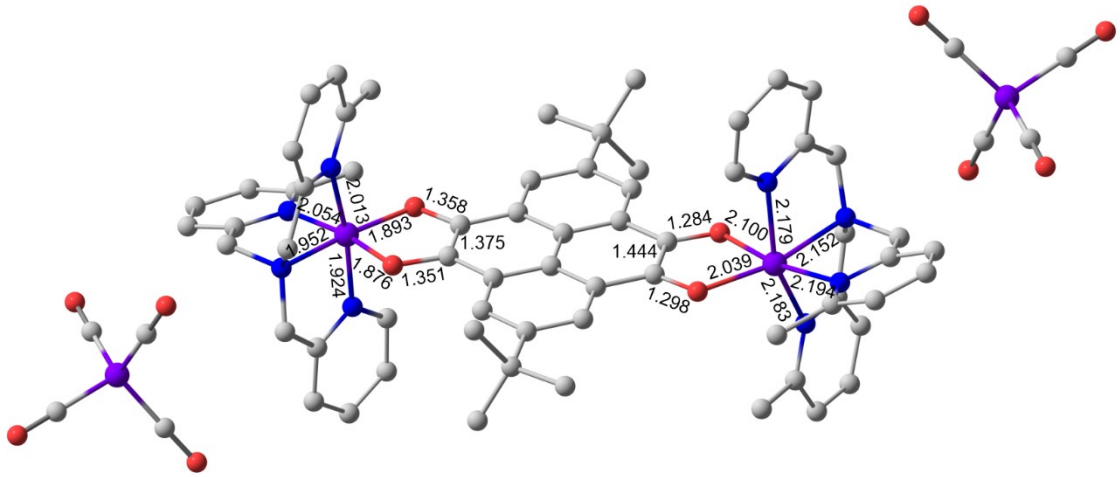

{ls-Co^{III}(Me_2tpa)–pyrene^{Cat-Sq}–hs-Co^{II}(Me_2tpa)}

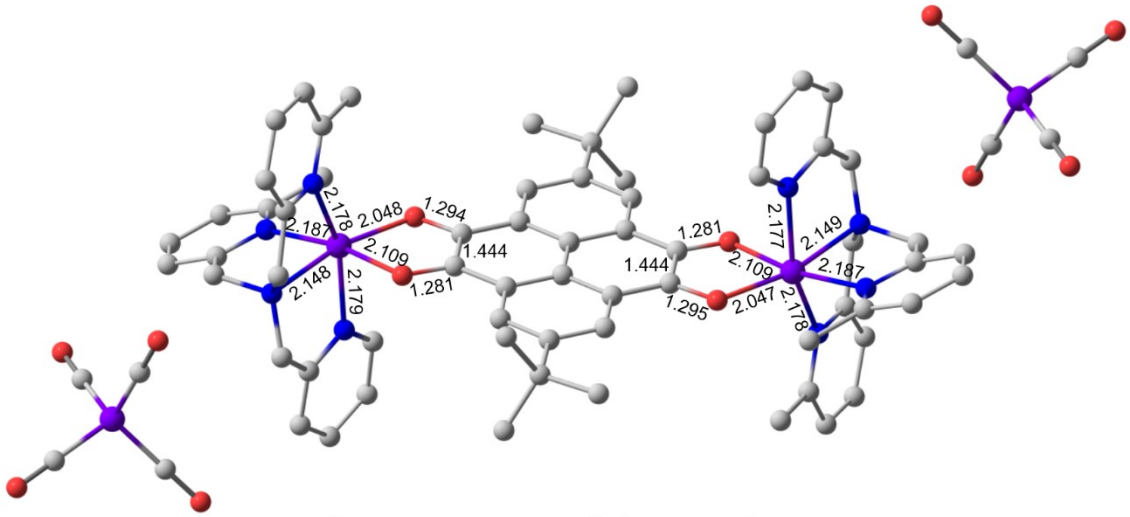

{hs-Co^{II}(Me_2tpa)–pyrene^{Sq-Sq}–hs-Co^{II}(Me_2tpa)}

Figure S20. Optimized geometries of the compound **5** in the three charge distributions, as calculated by the DFT UTPSSh/6-311++G(d,p) method.